



Lignin-rich sulfated wood nanofibers as high-performing adsorbents for the removal of lead and copper from water

Juho Antti Sirviö*, Miikka Visanko

Fibre and Particle Engineering Research Unit, University of Oulu, P.O. Box 4300, 90014, Oulu, Finland

ARTICLE INFO

Editor: Deyi Hou

Keywords:

Wood nanofibers
Sulfation
Lignin
Heavy metal
Adsorption

ABSTRACT

Lignin-rich wood nanofibers (WNFs) were investigated as adsorbents for heavy metals. Lignin-free cellulose nanofibers (CNFs) produced from bleached cellulose fibers were used as a reference. Two raw materials were used to produce WNFs: groundwood pulp as industrially produced wood fibers and sawdust as an abundantly available low-value industrial side stream. WNFs and reference CNFs were produced using a reactive deep eutectic solvent to obtain nanofibers with abundant sulfate groups on their surfaces. With a similar amount of sulfate groups, WNFs had a higher adsorbent performance compared to CNFs and, at low metal concentrations (0.24 mmol/l), the removal of both metals was almost quantitative with WNFs. However, it was noted that, at pHs 4 and 5, the sodium present in the buffer solution interfered with the adsorption, leading to lower adsorption capacities compared to the capacity at pH 3. In addition, in the case of lead, the adsorption capacity dramatically decreased at a high metal concentration, indicating that a high lead concentration results in the saturation of adsorption sites of sulfated nanofibers, leading to a decreased adsorption capacity. Nevertheless, it was observed that WNFs had a higher tolerance to high metal concentrations than CNFs.

1. Introduction

Pollution of land and water resources is one of the most prominent threats to humans, animals, and the ecosystem as whole. Although many toxic chemicals already exist in nature, they are widely spread via human activity. Pollutants can originate from industrial wastes or, for example, from the leaching of chemicals from mining fields (Ayangbenro and Babalola, 2017). In addition, everyday use of chemicals, such as drugs, can lead to the pollution of water resources (Bottoni et al., 2010).

Heavy metals are hazardous environmental pollutants due to their high toxicity and bioaccumulation (Yin et al., 2019). Although many heavy metals already exist in natural processes and are essential for most organisms, they generally have a very low toxic threshold, indicating that only a small excess can lead to a severe hazard (Jaishankar et al., 2014). Consequently, there exist strict limitations for the presence of heavy metals, for example, in drinking and industrial wastewaters (Ab Razak et al., 2015). To meet these limitations, many methods for the purification of heavy metal-containing waters have been investigated. Among them, adsorption has been widely investigated due to the easy operations, wide availability of different adsorbents, and reusability (Burakov et al., 2018; Yu et al., 2018a).

Cellulosic nanomaterials (e.g., cellulose nanocrystals [CNC] or

nanofibers [CNF]) are promising adsorbents for many environmental pollutants (Abouzeid et al., 2019; Voisin et al., 2017), including heavy metals (Sirviö et al., 2016; Hokkanen et al., 2013; Karim et al., 2017), dyes (Bai et al., 2019), and drugs (Selkälä et al., 2018). Due to the nanometric size (i.e., large surface area) and availability of various chemical modifications of cellulosic surfaces, cellulosic nanomaterials pose a high adsorption capacity comparable with that of commercial adsorbents. In contrast to other (nano)materials used for water treatment (Santhosh et al., 2016), cellulosic nanomaterials are renewable biomaterials exhibiting a low toxicity and thus themselves pose little environmental threat.

Although cellulosic nanomaterials are an efficient adsorbent for heavy metals, there is room for improvement. Thus far, most CNCs and CNFs used for water purification are obtained from purified cellulose sources, i.e., cellulose fibers where noncellulosic components (mainly lignin) have been removed. Especially in the case of wood cellulose fibers, intensive delignification and bleaching sequences are utilized to produce cellulose fibers. Lignin removal and the bleaching of the pulp is generally conducted using hazardous chemicals (i.e., chlorine-based oxidants). Therefore, it would be environmentally beneficial to produce water purification nanomaterials directly from wood fibers without or with mild chemical treatment. Further, the yield of wood fibers without chemical pulping is far greater compared to that of bleached cellulose

* Corresponding author.

E-mail address: juho.sirvio@oulu.fi (J.A. Sirviö).

<https://doi.org/10.1016/j.jhazmat.2019.121174>

Received 20 May 2019; Received in revised form 13 August 2019; Accepted 5 September 2019

Available online 06 September 2019

0304-3894/ © 2019 The Author(s). Published by Elsevier B.V. This is an open access article under the CC BY license (<http://creativecommons.org/licenses/by/4.0/>).

fibers.

In addition to the apparent advantages regarding the environmental friendliness, the presence of lignin could improve the removal efficiency of heavy metals. Lignin is conjugated polymer with a high consistency of aromatic groups that can interact with cations (Pillai and Rennekar, 2009), such as heavy metals. Moreover, the oxygen-containing groups (the hydroxyl, methoxy, and phenolic groups) are potential interaction sites of lignin for water purification (Naseer et al., 2019). Lignin isolated from various sources has been used in the removal of several heavy metals from water (Guo et al., 2008; Klapiszewski et al., 2015). However, there is scarce information on the use of lignin-rich WNFs in heavy metal adsorption. In the current research, the hypothesis of improved heavy metal removal with WNFs (lignin-rich) compared to CNFs (lignin-free) was studied. Two lignin-containing WNFs were produced from ground wood pulp (GWP) and sawdust, and their adsorption efficiency on lead and copper ions was studied. Lead and copper, which are both toxic and widely used in industrial processes were chosen as model metals, as they can be potentially present in waste-waters (Abdel-Halim et al., 2003; Foster et al., 1993). WNFs were produced using a reactive deep eutectic solvent (DES) to introduce sulfate ester groups on the wood fibers, followed by mild mechanical disintegration. The reference CNFs were produced in a similar method using bleached softwood dissolving pulp as a lignin-poor (< 0.5%) fiber source.

2. Materials and methods

2.1. Materials

Unbleached spruce GWP and sawdust were obtained in never-dried form, whereas the softwood dissolving cellulose pulp was obtained as dry sheets. The GWP and sawdust were first oven-dried (24 h at 60 °C) before use, and the dissolving pulp was first disintegrated in water and then filtered, washed with ethanol, and dried at 60 °C for 24 h in an oven. Before use, the sawdust was ground with an Ultra Centrifugal Mill ZM 200 (Retsch, Germany) using a sieve size of 250 µm. The lignin, acetone-soluble extractives, and hemicellulose and degraded cellulose contents of the raw materials were analyzed using TAPPI T 222 om-02, TAPPI T 280 standard pm-99, and TAPPI T 212 om-02 standards, respectively.

Urea (Borealis Biuron, Austria), sulfamic acid (Sigma-Aldrich, Germany), lead(II) nitrate (≥ 99.0%, Sigma-Aldrich), and copper(II) sulfate pentahydrate (98%, Sigma-Aldrich) were used as received. Additionally, 0.1/1 M NaOH and HCl (Merck), NaH₂PO₄ (Sigma-Aldrich), NaNO₃ (Sigma-Aldrich), NaCOO (Sigma-Aldrich), NaCH₃COO (OyFF Chemicals), Na₂HPO₄ (Sigma-Aldrich), NaHCO₃ (Merck), and Na₂CO₃ (Sigma-Aldrich) were used to prepare buffers. Polydiallyldimethylammonium chloride (polyDADMAC, BTG Müttek GmbH, Germany) was used as a polyelectrolyte titrant. For all steps requiring water, unless stated otherwise, deionized water was used.

2.2. Sulfation of wood and cellulose

Sulfation of wood and cellulose samples was performed according to our previous publication using DESs based on sulfamic acid and urea as reagent and reactions media (Sirviö et al., 2019; Sirviö and Visanko, 2019). Briefly, the DES components (8.99 g of sulfamic acid and 11.12 g of urea) were mixed together using a magnetic stirrer in an oil bath at 80 °C with a molar ratio (sulfamic acid:urea) of 1:2 until a clear solution was obtained. Then, GWP, ground sawdust, and dissolving pulp (1.5 g) were each separately added to the DES. The concentration of raw material in the DES was 6.9% (Sirviö et al., 2019). Next, the reaction temperature was increased to 150 °C, and the reaction was allowed to proceed for 30 min. The product was then filtrated and washed with water until the filtrate's pH was neutral. Finally, the product was collected and stored at 4 °C.

2.3. Elemental analysis of sulfated cellulose

The sulfated wood and cellulose samples were dried in an oven at 60 °C overnight. The nitrogen and sulfur contents of the samples were analyzed using the PerkinElmer CHNS/O 2400 Series II elemental and LECO CS-200 carbon-sulfur analyzers, respectively. The degree of substitution (DS) was calculated using Eq. (1) (Levdansky et al., 2014)

$$DS = \frac{S \times 162.15}{3206 - (S \times 97.10)} \quad (1)$$

where S represents the sulfur content, 162.15 the molecular weight (mmol/g) of the anhydroglucose unit, and 97.10 the molecular weight (mmol/g) of the ammonium sulfate group.

2.4. Disintegration of sulfated wood and cellulose into nanofibers

Disintegration of sulfated wood and cellulose was performed according to our previous publication. Briefly, sulfated wood and cellulose fibers in a consistency of 1 wt% and 0.5 wt%, respectively, were passed twice at a pressure of 1000 bar through the 400 and 200 µm chambers of a microfluidizer (Microfluidics M-110EH-30, USA). Disintegrated sulfated GWP, sawdust, and cellulose were named as sulfated wood nanofibers (SWNFs), sulfated sawdust nanofibers (SSDNFs), and sulfated cellulose nanofibers (SCNFs).

2.5. Lead and copper adsorption

Heavy metal containing model waters were prepared using either lead(II) nitrate or copper(II) sulfate pentahydrate to study the adsorption properties of the sulfated nanofibers. The experiments were performed in batch mode, and the performance of the nanofibers were evaluated in terms of pH (3–5), heavy metal content (0.24–7.61 mmol/l), and adsorption time (0.5–24 h). The sulfated nanofibers suspension (50 mg as a dry matter), lead/copper solution at desired concentration, 5 ml of pH buffer, and water were mixed to get a batch with a total weight of 25 g. The adsorption time was a standard 20 h for the experiments excluding the time series, and a constant heavy metal dose of 1.45 mmol/l was used, excluding the series with different concentrations. The adsorbed samples were filtered through a syringe filter with a pore size of 0.45 µm. The filtrates were collected, and the specimens' heavy metal concentrations were analyzed using an atom absorption spectrometer (AAS, Perkin Elmer 4100, USA). In addition to the experiment conducted using buffer solution, reference adsorption test was performed in similar manner described above, but the pH of the solution was adjusted using 30 wt% NH₂OH solution.

2.6. X-ray photoelectron spectroscopy (XPS)

Six films were fabricated by diluting the sulfated nanofibers suspension (50 mg as a dry matter) with water, followed by adjusting pH to 3, 4, or 5 using buffer solution. Specimens in different pHs were fabricated with or without the addition of lead (1.45 mmol/l) and mixed for 20 h prior to filtering the film on top of a membrane (pore size 0.45 µm). After the film formation, the samples were left to dry at room temperature. Samples were then analyzed using a Thermo Fisher Scientific ESCALAB 250Xi (UK) XPS equipped with a monochromatic AlKα X-ray source and operated at 300 W with a combination of electron flood gun and ion bombarding for charge compensation. The take-off angle was 45° in relation to the sample surface. The low-resolution survey scans were taken with a 1 eV step and 150 eV analyzer pass energy; high-resolution spectra were taken with a 0.1 eV step and 20 eV analyzer pass energy. All measurements were made in an ultra-high vacuum chamber pressure (5 × 10⁻⁹ mbar).

Table 1

Sulfate group content and anionic charge of nanofibers determined by polyelectrolyte titration.

Sample	Sulfate content (mmol/g)	Carbamate content (mmol/g)	Anionic charge (mmol/g)			
			pH			
			3	4	5	6
SWNF	3.1	1.2	2.01	2.01	2.03	2.04
SSDNF	3.1	1	2.12	2.12	2.15	2.15
SCNF	3.0	1.5	2.48	2.59	2.49	2.55

2.7. Charge density

The surface charge densities of the sulfated nanofibers were determined using the polyelectrolyte titration method through a particle charge detector (BTG Mutek PCD-03, Germany). 10 ml of nanofiber suspension (at 0.01 wt%) in buffer solution was titrated with polyDADMAC (1 meq/l). The charge density was calculated based on the polyDADMAC consumption.

3. Results and discussions

In this study, sulfated nanofibers were produced from two lignin-rich and one lignin-poor raw material, and the constitutions (cellulose, hemicellulose, lignin, and extractive contents) of these materials are presented in Table 1. The sulfation of GWP, sawdust, and bleached dissolving pulp was based on our previous publication (Sirviö et al., 2019; Sirviö and Visanko, 2019). With the applied methodology, the reactive hydroxyl groups in wood fibers react with sulfamic acid to produce ammonium salt of sulfuric acid ester (ammonium sulfate groups). In addition to sulfation, the formation of carbamate groups occurs due to the reaction of hydroxyl groups and urea. All the sulfated fibers had a high anionic sulfate group content and were easily disintegrated into nanosized fibers using two passes through the microfluidizer (the characterizations of SWNFs and CNFs are presented in previous publications (Sirviö et al., 2019; Sirviö and Visanko, 2019)).

According to the elemental analysis, all the samples contained similar sulfur and nitrogen contents, indicating that they had a similar reactivity and sulfate and carbamate group content. The charge density (determined using PE titration) of the SCNF was slightly higher compared to that of both wood-based nanofibers (Table 1). The SCNF's higher charge density could be due to the slightly different morphology between wood-based and cellulose-based nanofibers. Although most of the nanofibers in the SWNF and SSDNF were in the range of a few nanometers (average diameter of 3 nm), some larger nanofiber aggregates were observed. In the case of the SCNF, large aggregates were absent. In addition, some irregularly shaped lignin- and hemicellulose-based nanoparticles were present in the SWNF and SSDNF. Due to the different nanoparticles' morphology, the interaction between the polymeric titrant and the nanoparticles might vary in different samples. On the other hand, all the samples showed similar behavior in the function of pH, i.e., the charge density remained unchanged at the studied pH range (3–6). Independence of the charge density from the pH demonstrates the high acidity of the sulfate groups, since they are protonated even at a low pH.

3.1. Effect of pH on the adsorption of copper and lead

The adsorption capacity of all the samples on both copper and lead was found to be the highest at a low pH (Fig. 1). For copper, the adsorption efficiency remained similar at a pH range of 3–4 for the SWNFs and SCNFs (Fig. 1a). On the other hand, a small drop in the adsorption capacity was observed with the SSDNF at pH 4. In the case of lead, the adsorption capacity decreased with all samples when the pH increased

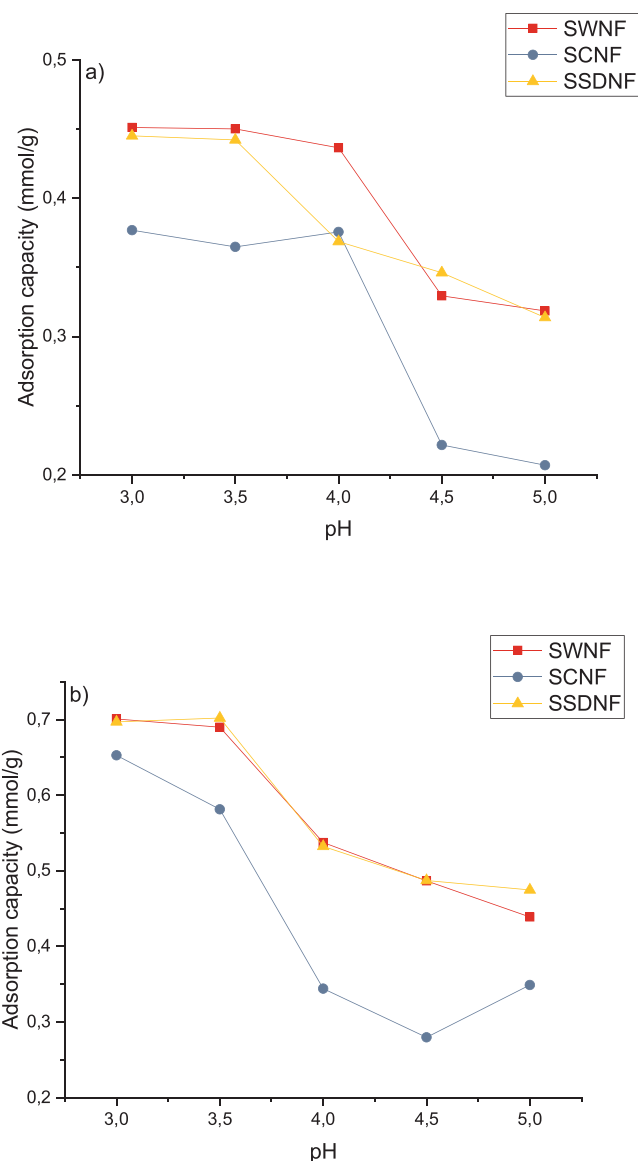


Fig. 1. Adsorption capacities of sulfated nanofibers on a) copper and b) lead as a function of pH. Initial concentration of copper and lead were 1.49 mmol/g and 0.95 mmol/g, respectively.

from 3.5 to 5 (Fig. 1b). The results obtained at various pHs were somewhat contradictory to previously published studies of the adsorption of lead and other metals using sulfonated wheat pulp nanofibers (Suopajarvi et al., 2015) and carboxylated cellulosic nanomaterials (Yu et al., 2013; Kardam et al., 2013; Sehaqui et al., 2014). In previous studies, the adsorption capacity generally increased as a function of increased pH. However, the removal of both lead and copper by sulfated nanofibers remained at a relative good level even at the highest pH studied: around 60% for lignin-containing nanofibers and around 45% for SCNFs. It should be noted that, due to the precipitation of metals at higher pHs, adsorption studies are generally conducted at a pH below seven.

As a result of the pH experiments, the adsorption capacities of the lignin-containing nanofibers were recorded as higher than the SCNFs' for both metals (Fig. 1). All the samples had somewhat similar substitution patterns (i.e., sulfate and carbamate group content), thus it was most likely that the lignin present in the SWNFs and SSDNFs contributed to the adsorption process. Due to the cation- π interaction (Pillai and Rennecker, 2009) and the presence of phenolic groups (Yu et al., 2000), lignin can interact with various metals. This lignin-metal

interaction then contributes to the higher adsorption capacity of lignin-containing nanofibers compared to that of the nanofibers produced from bleached cellulose pulp where lignin was removed.

Due to the possible chemical modification of lignin (sulfation of phenolic groups), the determination of the sulfated wood samples' lignin content could not be conducted. However, the yields of both sulfated GWP and sawdust were over 90% (Sirviö and Visanko, 2019). Therefore, it can be assumed that most of the original lignin remained in the sulfated samples, which was seen as a good absorption capacity. It is also noteworthy to consider the yield of sulfated bleached pulp, which was 75%. The higher yields of sulfated GWP and sawdust compared to that of dissolving pulp further demonstrate the advantage of using nonbleached raw materials for the preparation of heavy metal absorbents.

3.2. XPS studies on the adsorption mechanism at function of pH

For more detailed insight about the effect of the pH on the adsorption, SWNF films were produced with and without lead using vacuum filtration. The films' surface was then analyzed with XPS. It was observed that the amount of lead on the films was higher when the film was produced at pH 3 (Table 2), which is in line with adsorption capacity studies (Fig. 1) (survey spectra of films are presented in Supplementary Information). At pH 3, no elements other than C, O, N, S, and Pb were observed on the film surfaces. However, at pHs 4 and 5, the presence of sodium was observed. The sodium ion originates from the buffer solution used during the adsorption studies. Therefore, it might be that the sodium ion interferes with the adsorption of lead from water due to the exchange of the ammonium into sodium. The amount of sodium on the films' surface was lower in the presence of lead due to the competing ion exchange of ammonium ion with sodium and lead.

The impact of sodium was studied with an additional lead adsorption test using SWNFs while maintaining pH at 5 using aqueous NH_4OH . The adsorption capacity (0.66 mmol/g) at pH 5 using NH_4OH was similar to that obtained at pH 3 in the previous tests (0.70 mmol/g) and in contrast to the results recorded using the buffer solution (0.43 mmol/g). It can be assumed that the presence of additional ions (here, sodium) in the solution has an important effect on the heavy metals adsorption capacity of the sulfated nanofibers. As the main aim of current study is to investigate the effect of lignin on these adsorption properties, further studies were done using a pH 3 buffer. However, future studies should be conducted to investigate the adsorption behavior in the presence of other ions (e.g., using real wastewaters).

3.3. Effect of time on the adsorption of copper and lead

The adsorption of both metals was a fast reaction, as the maximum adsorption capacity was already obtained for all the samples after half an hour (Fig. 2). This is in line with the previous studies of lead adsorption on sulfonated nanocelluloses (Suopajarvi et al., 2015). This fast adsorption was due to the nanofibers' large surface area as well as

Table 2

Elemental constitution determined with XPS for SWNF films prepared in different pHs with and without lead.

Sample	pH	Elements					
		C1s	O1s	N1s	S2p	Pb4f	Na1s
SWNFs	3	41.93	42.94	5.39	9.75	- ^a	- ^a
	4	50.5	35.26	2.39	8.68	- ^a	3.17
	5	53.93	34.77	4.1	4.52	- ^a	2.68
SWNFs with lead	3	30.14	34.03	2.61	15.07	18.15	- ^a
	4	35.95	34.97	2.73	13.23	11.2	1.92
	5	50.04	36.86	3.41	6.95	0.86	1.87

^a Not detected.

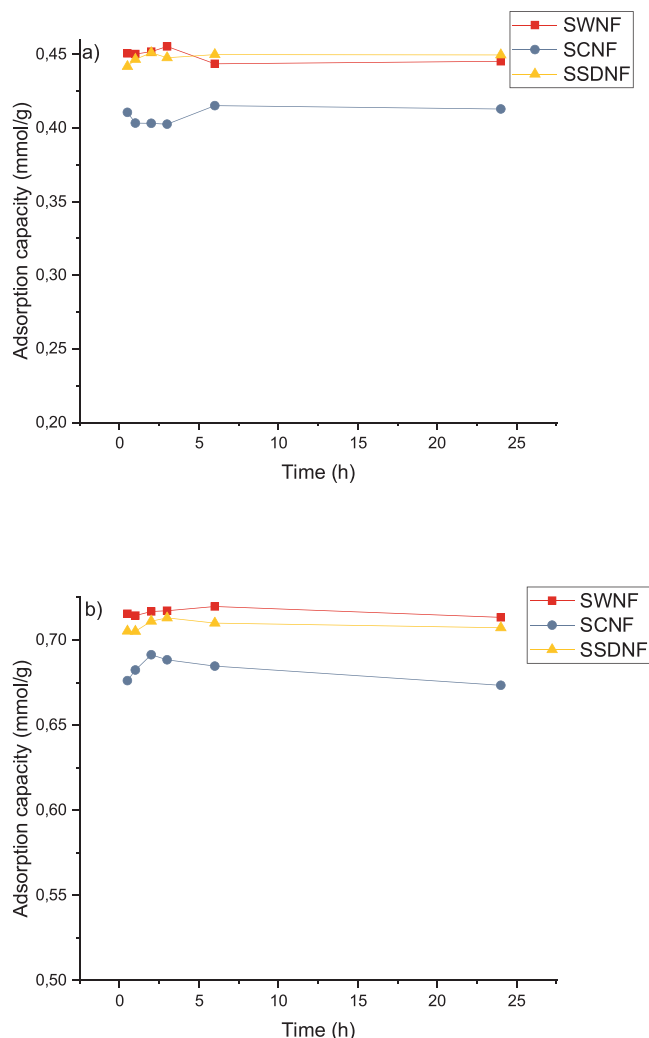


Fig. 2. Adsorption capacities of sulfated nanofibers on a) copper and b) lead as a function of adsorption time. Initial concentration of copper and lead were 1.49 mmol/g and 0.95 mmol/g, respectively.

the presence of a substantial number of absorption sites (i.e., sulfate groups) on the surface. In previous studies, a fast adsorption response has been reported for cellulosic nanomaterials in the absorption of various water contaminants (Hokkanen et al., 2013; Liu et al., 2015).

3.4. Effect of initial metal concentration on the adsorption of copper and lead

The adsorption capacity for all the samples increased when the initial amount of copper was increased from 0.24 to 7.61 mmol/g (Fig. 3a). This is well-known behavior, as the increase in the metal concentration increases the possible interaction between metal and the adsorbent, resulting in a higher adsorption capacity. However, the highest absorption percentages were obtained at a lower metal concentration (0.24 mmol/g), where 97% of the copper was removed with SWNFs and SSDNFs (Fig. 3b). A lower efficiency (87%) was obtained using SCNFs. The high absorption percentage at a low metal concentration is important in real-life applications, as metals typically exist in minute quantities in wastewaters (Karvelas et al., 2003).

The calculation from the data of the adsorption isotherm of copper at various concentrations showed a better fit to the Freundlich isotherm compared to the Langmuir. This suggests the presence of heterogeneous adsorption sites in all the samples. This might be explained by the assumption that both sulfate and carbamate groups contributed to the

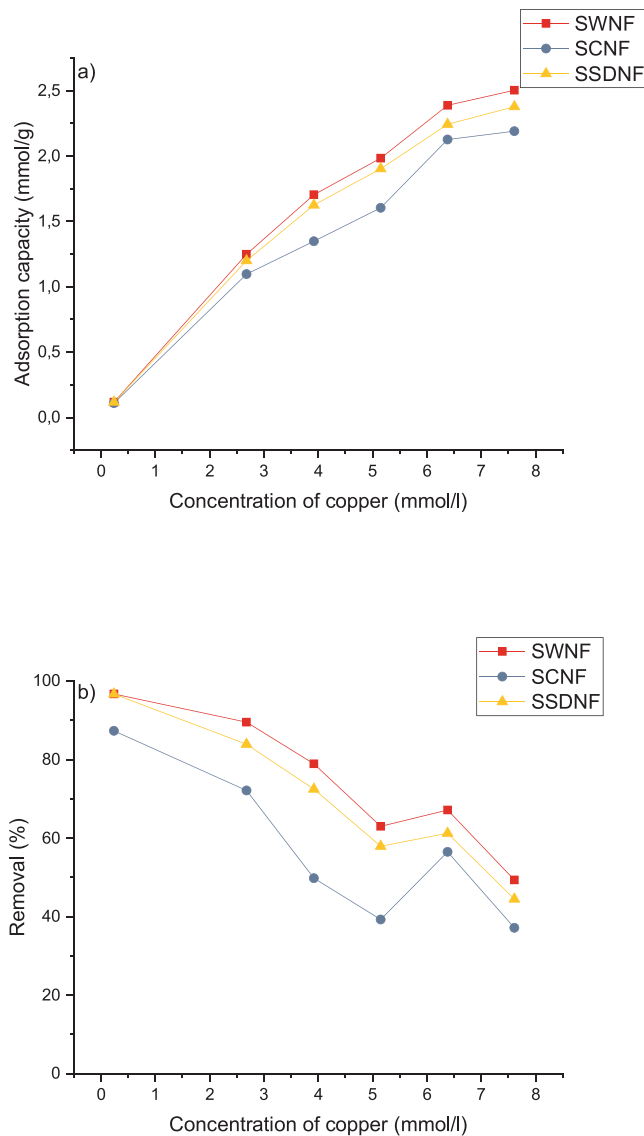


Fig. 3. a) Adsorption capacities of sulfated nanofibers and b) removal percentage as a function of copper concentration.

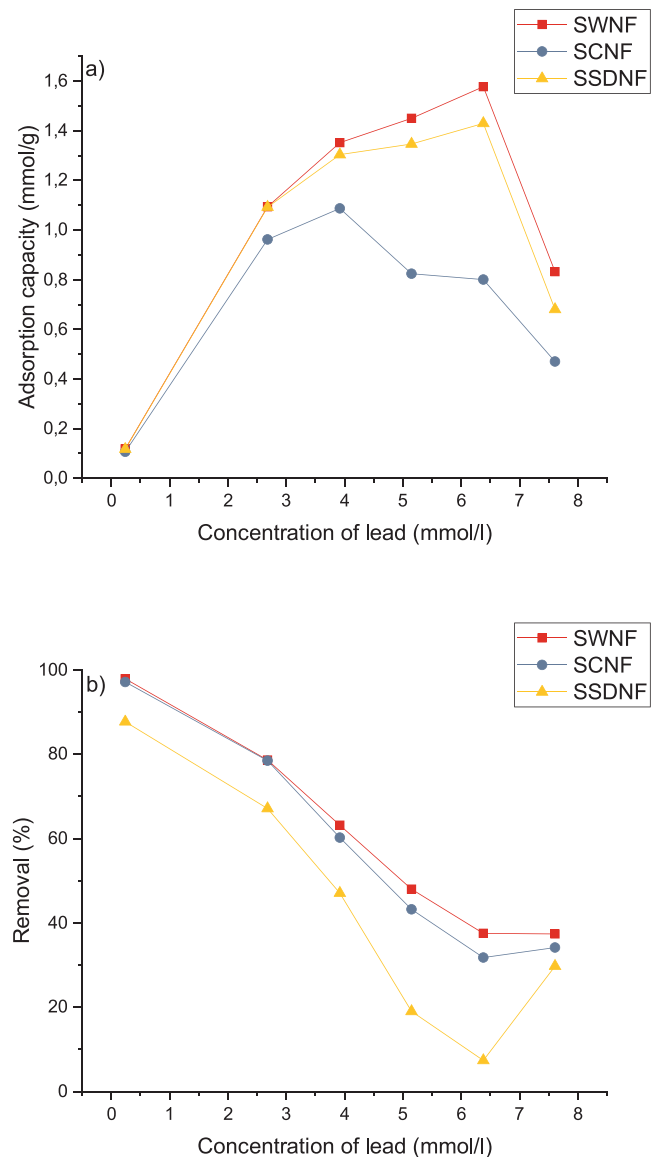


Fig. 4. a) Adsorption capacities of sulfated nanofibers and b) removal percentage as a function of lead concentration.

Table 3

Adsorption capacities of copper by cellulosic nanomaterials.

Nanocellulose	Modification (functionality)	Maximum adsorption capacity (mmol/g)	Ref
CNC	TEMPO-oxidation (-COO ⁻)	0.23	(Hamid et al., 2016)
	Periodate + chlorite oxidation (-COO ⁻)	2.91	(Sheikhi et al., 2015)
	Phosphorylation (-PO ₃ ²⁻)	1.84	(Liu et al., 2015)
	Sulfation (-SO ₃ ⁻)	0.31	(Liu et al., 2015)
CNF	TEMPO-oxidation (-COO ⁻)	2.10	(Sehaqui et al., 2014)
	Succination (-COO ⁻)	1.9	(Hokkanen et al., 2013)
	Amination (-NH ₂)	3.15	(Hokkanen et al., 2014)
	Phosphorylation (-PO ₃ ²⁻)	1.79	(Liu et al., 2015)
	Sulfation (-SO ₃ ⁻)	2.20 ^a	This work
BC ^b	Amination (-NH ₂ , -NH ₂)	0.99	(Shen et al., 2009)
	Carboxymethylation (-COO ⁻)	0.32	(Chen et al., 2009)
WNF	Sulfation (-SO ₃ ⁻)	2.50 ^a	This work
	Sulfation (-SO ₃ ⁻)	2.20 ^a	(from GWP) This work (from sawdust)

^a Experimental value.

^b Bacterial cellulose.

Table 4
Adsorption capacities of lead by cellulosic nanomaterials.

Nanocellulose	Modification (functionality)	Maximum adsorption capacity (mmol/g)	Ref
CNC	Succination (-COO ⁻)	2.24	(Yu et al., 2013)
	Sulfation (-SO ₃ ⁻)	0.05	(Kardam et al., 2013)
CNF	TEMPO-oxidation/thiolation (-COO ⁻ /-SH)	0.66	(Yang et al., 2014)
	Sulfonation (-SO ₃ ⁻)	1.2	(Suopajärvi et al., 2015)
	Sulfation (-SO ₃ ⁻)	1.1 ^a	This work
BC ^b	Amination (-NH ₂ , -NH ₂)	0.42	(Shen et al., 2009)
	Carboxymethylation (-COO ⁻)	0.32	(Chen et al., 2009)
	Polyethyleneimine-grafting (-NH ₂ , -NH ₂)	0.60	(Jin et al., 2017)
WNF	Sulfation (-SO ₃ ⁻)	1.60 ^a	This work (from GWP)
	Sulfation (-SO ₃ ⁻)	1.40 ^a	This work (from sawdust)

^a Experimental value.

^b Bacterial cellulose.

adsorption process with different adsorption rates. In addition to the ion exchange of metal ions with negatively charged sulfate groups, carbamate groups can act as a chelating agent for metal ions (Guo et al., 2006).

The maximum experimental adsorption capacity of the SWNFs, SDNFs, and SCNFs, were 2.5, 2.4, and 2.2 mmol/g, respectively. These values are among the highest capacities reported for the adsorption of copper with cellulosic nanomaterials (Table 3) (Abouzeid et al., 2019). A higher adsorption capacity compared to sulfated nanofibers has been reported with electrosterically stabilized CNCs (2.9 mmol/g) (Sheikhi et al., 2015) and aminated CNFs (3.15 mmol/g), whereas the adsorption capacities of 1.8 and 2.1 mmol/g were obtained using phosphorylated CNCs (Liu et al., 2015) and carboxylated CNFs (Sehaqui et al., 2014), respectively. The adsorption capacities of the sulfated nanofibers were also higher compared to that of many clay minerals (Uddin, 2017). Among the highest adsorption capacity (0.85 mmol/g) for clay minerals was reported for immobilized bentonite (Erdem et al., 2009). On the other hand, carbon-based adsorbents have shown superior adsorption capacities (Yang et al., 2019). For example, an adsorption capacity of 3.46 mmol/g was obtained with carbonaceous nanofiber/Ni-Al layered double hydroxide nanocomposites (Yu et al., 2018b), and an adsorption capacity of copper as high as 26.6 mmol/g has been reported for a polyvinylpyrrolidone-reduced graphene oxide-based adsorbent (Zhang et al., 2014).

3.5. Effect of initial metal concentration on the adsorption of copper

Compared to copper, the nanofibers' adsorption capacity on lead showed a different behavior as a function of initial metal concentration. In the SWNFs' and SSDNFs' case, the adsorption capacity gradually increased when the initial lead concentration increased from 0.24 to 6.38 mmol/g (Fig. 4a). When the lead concentration further increased to 7.61 mmol/g, the adsorption capacity dropped significantly (from around 1.4 mmol/g to close to 0.8 mmol/g). In the SCNFs' case, a drop in the adsorption capacity was already observed at a lead concentration of 5.15 mmol/g. On the other hand, the absorption percentage was similar to copper's, i.e., the highest removal was observed at a concentration of 0.24 mmol/g. At this concentration, the absorption percentages with SWNFs and SSDNFs were 98 and 97%, respectively, whereas SCNFs removed 88% of the lead (Fig. 4b).

The SWNFs' and SSDNFs' maximum experimental adsorption capacities were 1.6 and 1.4 mmol/g, respectively. This was close to the lead:sulfate group molar ratio of 1:2. In the CNFs' case, the maximum experimental adsorption capacity was somewhat lower (1.1 mmol/g) but still close to the same lead:sulfate molar ratio than in lignin-containing nanofibers. This might indicate that the main adsorption sites (sulfate groups) were saturated at a high lead concentration when the two monovalent sulfate groups interacted with the divalent lead ion.

This interaction might lead to the crosslinking of the sulfated nanofibers at a high lead concentration, leading to a decrease in adsorption efficiency. As the nanofibers' high adsorption capacity was assumed to be due to the nanometric size, and thus large surface area, the crosslinking can decrease the adsorption efficiency by forming agglomerates, which then decreases the active surface area. A higher lead concentration to achieve the saturation point with SWNFs and SSDNFs was most likely due to the presence of lignin, which can also participate in the lead adsorption. The decrease of adsorption capacity was not observed with copper (lead and copper had an oxidation of II), indicating that copper ions had a tendency to form a metal-sulfate complex with other than a 1:2 M ratio.

Similar to copper, the Freundlich isotherm was found to be more preferable in the adsorption of lead on sulfated nanofibers. However, as the lead adsorption was observed to decrease at higher lead concentrations, the adsorption isotherm calculations might not be entirely reliable.

The SCNFs' experimental adsorption capacity was 1.1 mmol/g, which was lower compared to that of the SWNFs (1.6 mmol/g) and SSDNFs (1.4 mmol/g). The adsorption capacities of SWNFs and SSDNFs were also in line with the highest maximum adsorption capacities obtained in the literature for lead using cellulosic nanomaterials (Table 4) (Abouzeid et al., 2019). Succinylated CNCs have been shown to exhibit an adsorption capacity of 2.2 mmol/g (Yu et al., 2013), and a similar adsorption capacity was observed with hydrogel beads produced from carboxylated CNCs and alginate (Hu et al., 2018). Similar to copper adsorption, the adsorption capacity of sulfated nanofibers was generally higher compared to that obtained with clay minerals (Uddin, 2017). However, an adsorption capacity of 39.2 mmol/g has been obtained using modified multiwalled carbon nanotubes (Alizadeh et al., 2016).

4. Conclusions

It was demonstrated that sulfated nanofibers produced from two separate lignin-rich sources (GWP and sawdust) exhibited the higher adsorption capacities of both copper and lead in model waters compared to their counterpart nanofibers obtained from bleached cellulose pulp. As both lignin-containing nanofibers and CNFs contained similar amounts of active functional groups (i.e., sulfate and carbamate groups), the results indicated that lignin participated in the metal removal. Both sulfate and carbamate groups in sulfated nanofibers take part in the metal removal by ion exchange and chelation, respectively, whereas high adsorption capacities of SWNFs and SSDNFs were due to the interaction of metals with aromatic and phenolic groups of lignin. Moreover, the yield of sulfated wood fibers was significantly higher compared to that of sulfated bleached cellulose fibers. Together with the advantage of raw materials (e.g., the utilization of a low amount of toxic chemicals and a higher yield), lignin-containing nanofibers had a

significantly higher potential in water treatment applications compared to more traditional CNFs. Furthermore, the adsorption capacities of sulfated nanofibers were among the highest values reported for cellulosic nanomaterials in the literature. However, it was observed that the sodium ion presented in the buffer solution interfered with the adsorption of metals. Therefore, future studies should be conducted with the presence of other metal ions (e.g., using real wastewaters). In addition, regeneration and reuse of lignin-containing adsorbents should be researched to demonstrate the full potential of these functional wood-based materials.

Acknowledgments

We acknowledge Elisa Wirkkala and Dr. Mika Kaakinen for their assistance in the elemental analysis and TEM measurements, respectively. The research was conducted as part of the ARVOPURU project funded by the Council of Oulu Region, which was granted by the European Regional Development Fund of the European Union.

Appendix A. Supplementary data

Supplementary material related to this article can be found, in the online version, at doi:<https://doi.org/10.1016/j.jhazmat.2019.121174>.

References

- Ab Razak, N.H., Praveena, S.M., Aris, A.Z., Hashim, Z., 2015. Drinking water studies: a review on heavy metal, application of biomarker and health risk assessment (a special focus in Malaysia). *J. Epidemiol. Glob. Health* 5, 297–310. <https://doi.org/10.1016/j.jegh.2015.04.003>.
- Abdel-Halim, S.H., Shehata, A.M.A., El-Shahat, M.F., 2003. Removal of lead ions from industrial waste water by different types of natural materials. *Water Res.* 37, 1678–1683. [https://doi.org/10.1016/S0043-1354\(02\)00554-7](https://doi.org/10.1016/S0043-1354(02)00554-7).
- Abouzeid, R.E., Khiari, R., El-Wakil, N., Dufresne, A., 2019. Current state and new trends in the use of cellulose nanomaterials for wastewater treatment. *Biomacromolecules* 20, 573–597. <https://doi.org/10.1021/acs.biomac.8b00839>.
- Alizadeh, B., Ghorbani, M., Salehi, M.A., 2016. Application of polyrhodanine modified multi-walled carbon nanotubes for high efficiency removal of Pb(II) from aqueous solution. *J. Mol. Liq.* 220, 142–149. <https://doi.org/10.1016/j.molliq.2016.04.065>.
- Ayangbenro, A.S., Babalola, O.O., 2017. A new strategy for heavy metal polluted environments: a review of microbial biosorbents. *Int. J. Environ. Res. Public Health* 14, 94. <https://doi.org/10.3390/ijerph14010094>.
- Bai, L., Liu, Y., Ding, A., Ren, N., Li, G., Liang, H., 2019. Fabrication and characterization of thin-film composite (TFC) nanofiltration membranes incorporated with cellulose nanocrystals (CNCs) for enhanced desalination performance and dye removal. *Chem. Eng. J.* 358, 1519–1528. <https://doi.org/10.1016/j.cej.2018.10.147>.
- Bottoni, P., Caroli, S., Caracciolo, A.B., 2010. Pharmaceuticals as priority water contaminants. *Toxicol. Environ. Chem.* 92, 549–565. <https://doi.org/10.1080/02722241003614320>.
- Burakov, A.E., Galunin, E.V., Burakova, I.V., Kucherova, A.E., Agarwal, S., Tkachev, A.G., Gupta, V.K., 2018. Adsorption of heavy metals on conventional and nanostructured materials for wastewater treatment purposes: a review. *Ecotoxicol. Environ. Saf.* 148, 702–712. <https://doi.org/10.1016/j.ecoenv.2017.11.034>.
- Chen, S., Zou, Y., Yan, Z., Shen, W., Shi, S., Zhang, X., Wang, H., 2009. Carboxymethylated-bacterial cellulose for copper and lead ion removal. *J. Hazard. Mater.* 161, 1355–1359. <https://doi.org/10.1016/j.jhazmat.2008.04.098>.
- Erdem, B., Özcan, A., Gök, Ö., Özcan, A.S., 2009. Immobilization of 2,2'-dipyridyl onto bentonite and its adsorption behavior of copper(II) ions. *J. Hazard. Mater.* 163, 418–426. <https://doi.org/10.1016/j.jhazmat.2008.06.112>.
- Foster, N.S., Noble, R.D., Koval, C.A., 1993. Reversible photoreductive deposition and oxidative dissolution of copper ions in titanium dioxide aqueous suspensions. *Environ. Sci. Technol.* 27, 350–356. <https://doi.org/10.1021/es00039a016>.
- Guo, X., Zhang, S., Shan, X., 2008. Adsorption of metal ions on lignin. *J. Hazard. Mater.* 151, 134–142. <https://doi.org/10.1016/j.jhazmat.2007.05.065>.
- Guo, L., Zhang, S.-F., Ju, B.-Z., Yang, J.-Z., 2006. Study on adsorption of Cu(II) by water-insoluble starch phosphate carbamate. *Carbohydr. Polym.* 63, 487–492. <https://doi.org/10.1016/j.carbpol.2005.10.006>.
- Hamid, H.A., Jenidi, Y., Thielemans, W., Somerfield, C., Gomes, R.L., 2016. Predicting the capability of carboxylated cellulose nanowhiskers for the remediation of copper from water using response surface methodology (RSM) and artificial neural network (ANN) models. *Ind. Crops Prod.* 93, 108–120. <https://doi.org/10.1016/j.indcrop.2016.05.035>.
- Hokkanen, S., Repo, E., Sillanpää, M., 2013. Removal of heavy metals from aqueous solutions by succinic anhydride modified mercerized nanocellulose. *Chem. Eng. J.* 223, 40–47. <https://doi.org/10.1016/j.cej.2013.02.054>.
- Hokkanen, S., Repo, E., Suopajarvi, T., Liimatainen, H., Niinimäki, J., Sillanpää, M., 2014. Adsorption of Ni(II), Cu(II) and Cd(II) from aqueous solutions by amino modified nanostructured microfibers. *Cellulose* 21, 1471–1487. <https://doi.org/10.1007/s10570-014-0240-4>.
- Hu, Z.-H., Omer, A.M., Ouyang, X., Yu, D., 2018. Fabrication of carboxylated cellulose nanocrystal/sodium alginate hydrogel beads for adsorption of Pb(II) from aqueous solution. *Int. J. Biol. Macromol.* 108, 149–157. <https://doi.org/10.1016/j.jbiomac.2017.11.171>.
- Jaishankar, M., Tseten, T., Anbalagan, N., Mathew, B.B., Beeregowda, K.N., 2014. Toxicity, mechanism and health effects of some heavy metals. *Interdiscip. Toxicol.* 7, 60–72. <https://doi.org/10.2478/interdiscip-2014-0009>.
- Jin, X., Xiang, Z., Liu, Q., Chen, Y., Lu, F., 2017. Polyethyleneimine-bacterial cellulose bioadsorbent for effective removal of copper and lead ions from aqueous solution. *Bioresour. Technol.* 244, 844–849. <https://doi.org/10.1016/j.biortech.2017.08.072>.
- Kardam, A., Raj, K.R., Srivastava, S., Srivastava, M.M., 2013. Nanocellulose fibers for biosorption of cadmium, nickel, and lead ions from aqueous solution. *Clean Technol. Environ. Policy* 16, 385–393. <https://doi.org/10.1007/s10098-013-0634-2>.
- Karim, Z., Hakalahti, M., Tammelin, T., Mathew, A.P., 2017. In situ TEMPO surface functionalization of nanocellulose membranes for enhanced adsorption of metal ions from aqueous medium. *RSC Adv.* 7, 5232–5241. <https://doi.org/10.1039/C6RA25707K>.
- Karvelas, M., Katsoyiannis, A., Samara, C., 2003. Occurrence and fate of heavy metals in the wastewater treatment process. *Chemosphere* 53, 1201–1210. [https://doi.org/10.1016/S0045-6535\(03\)00591-5](https://doi.org/10.1016/S0045-6535(03)00591-5).
- Klapiszewski, L., Bartczak, P., Wysokowski, M., Jankowska, M., Kabat, K., Jesionowski, T., 2015. Silica conjugated with kraft lignin and its use as a novel 'green' sorbent for hazardous metal ions removal. *Chem. Eng. J.* 260, 684–693. <https://doi.org/10.1016/j.cej.2014.09.054>.
- Levdansky, V.A., Kondracenko, A.S., Levdansky, A.V., Kuznetsov, B.N., Djakovitch, L., Pinel, C., Левданский, В.А., Кондрасенко, А.С., Левданский, А.В., Кузнецов, Б.Н., Дьякович, Л., Пинель, К., 2014. Sulfation of Microcrystalline Cellulose with Sulfamic Acid in N,N-Dimethylformamide and Diglyme, Сульфатирование микрокристаллической целлюлозы сульфаминовой кислотой в N,N-диметилформамиде и диглиме. <http://elib.sfu-kras.ru/handle/2311/13248> (Accessed 27 September 2017).
- Liu, P., Borrell, P.F., Božič, M., Kokol, V., Oksman, K., Mathew, A.P., 2015. Nanocelluloses and their phosphorylated derivatives for selective adsorption of Ag⁺, Cu²⁺ and Fe³⁺ from industrial effluents. *J. Hazard. Mater.* 294, 177–185. <https://doi.org/10.1016/j.jhazmat.2015.04.001>.
- Naseer, A., Jamshaid, A., Hamid, A., Muhammad, N., Ghauri, M., Iqbal, J., Rafiq, S., khuram, S., Shah, N.S., 2019. Lignin and lignin based materials for the removal of heavy metals from waste water-an overview. *Z. Für Phys. Chem.* 233, 315–345. <https://doi.org/10.1515/zpch-2018-1209>.
- Pillai, K.V., Rennecker, S., 2009. Cation- π interactions as a mechanism in technical lignin adsorption to cationic surfaces. *Biomacromolecules* 10, 798–804. <https://doi.org/10.1021/bm801284y>.
- Santhosh, C., Velmurugan, V., Jacob, G., Jeong, S.K., Grace, A.N., Bhatnagar, A., 2016. Role of nanomaterials in water treatment applications: a review. *Chem. Eng. J.* 306, 1116–1137. <https://doi.org/10.1016/j.cej.2016.08.053>.
- Sehaqui, H., de Larraya, U.P., Liu, P., Pfenninger, N., Mathew, A.P., Zimmermann, T., Tingaut, P., 2014. Enhancing adsorption of heavy metal ions onto biobased nanofibers from waste pulp residues for application in wastewater treatment. *Cellulose* 21, 2831–2844. <https://doi.org/10.1007/s10570-014-0310-7>.
- Selkälä, T., Suopajarvi, T., Sirviö, J.A., Luukkonen, T., Lorite, G.S., Kalliola, S., Sillanpää, M., Liimatainen, H., 2018. Rapid uptake of pharmaceutical salbutamol from aqueous solutions with anionic cellulose nanofibrils: the importance of pH and colloidal stability in the interaction with ionizable pollutants. *Chem. Eng. J.* 350, 378–385. <https://doi.org/10.1016/j.cej.2018.05.163>.
- Sheikhi, A., Safari, S., Yang, H., van de Ven, T.G.M., 2015. Copper removal using electrosterically stabilized nanocrystalline cellulose. *ACS Appl. Mater. Interfaces* 7, 11301–11308. <https://doi.org/10.1021/acsami.5b01619>.
- Shen, W., Chen, S., Shi, S., Li, X., Zhang, X., Hu, W., Wang, H., 2009. Adsorption of Cu(II) and Pb(II) onto diethylenetriamine-bacterial cellulose. *Carbohydr. Polym.* 75, 110–114. <https://doi.org/10.1016/j.carbpol.2008.07.006>.
- Sirviö, J.A., Visanko, M., 2019. Highly transparent nanocomposites based on poly(vinyl alcohol) and sulfated UV-absorbing wood nanofibers. *Biomacromolecules* 20, 2413–2420. <https://doi.org/10.1021/acs.biomac.9b00427>.
- Sirviö, J.A., Hasa, T., Leiviskä, T., Liimatainen, H., Hormi, O., 2016. Bisphosphonate nanocellulose in the removal of vanadium(V) from water. *Cellulose* 23, 689–697. <https://doi.org/10.1007/s10570-015-0819-4>.
- Sirviö, J.A., Ukkola, J., Liimatainen, H., 2019. Direct sulfation of cellulose fibers using a reactive deep eutectic solvent to produce highly charged cellulose nanofibers. *Cellulose* 26, 2303–2316. <https://doi.org/10.1007/s10570-019-02257-8>.
- Suopajarvi, T., Liimatainen, H., Karjalainen, M., Uppala, H., Niinimäki, J., 2015. Lead adsorption with sulfonated wheat pulp nanocelluloses. *J. Water Process Eng.* 5, 136–142. <https://doi.org/10.1016/j.jwpe.2014.06.003>.
- Uddin, M.K., 2017. A review on the adsorption of heavy metals by clay minerals, with special focus on the past decade. *Chem. Eng. J.* 308, 438–462. <https://doi.org/10.1016/j.cej.2016.09.029>.
- Voisin, H., Bergström, L., Liu, P., Mathew, A.P., 2017. Nanocellulose-based materials for water purification. *Nanomaterials* 7. <https://doi.org/10.3390/nano7030057>.
- Yang, X., Wan, Y., Zheng, Y., He, F., Yu, Z., Huang, J., Wang, H., Ok, Y.S., Jiang, Y., Gao, B., 2019. Surface functional groups of carbon-based adsorbents and their roles in the removal of heavy metals from aqueous solutions: a critical review. *Chem. Eng. J.* 366, 608–621. <https://doi.org/10.1016/j.cej.2019.02.119>.
- Yang, R., Aubrecht, K.B., Ma, H., Wang, R., Grubbs, R.B., Hsiao, B.S., Chu, B., 2014. Thiol-modified cellulose nanofibrous composite membranes for chromium (VI) and lead (II) adsorption. *Polymer* 55, 1167–1176. <https://doi.org/10.1016/j.polymer.2014.01.043>.

- Yin, K., Wang, Q., Lv, M., Chen, L., 2019. Microorganism remediation strategies towards heavy metals. *Chem. Eng. J.* 360, 1553–1563. <https://doi.org/10.1016/j.cej.2018.10.226>.
- Yu, X., Tong, S., Ge, M., Wu, L., Zuo, J., Cao, C., Song, W., 2013. Adsorption of heavy metal ions from aqueous solution by carboxylated cellulose nanocrystals. *J. Environ. Sci.* 25, 933–943. [https://doi.org/10.1016/S1001-0742\(12\)60145-4](https://doi.org/10.1016/S1001-0742(12)60145-4).
- Yu, B., Zhang, Y., Shukla, A., Shukla, S.S., Dorris, K.L., 2000. The removal of heavy metal from aqueous solutions by sawdust adsorption — removal of copper. *J. Hazard. Mater.* 80, 33–42. [https://doi.org/10.1016/S0304-3894\(00\)00278-8](https://doi.org/10.1016/S0304-3894(00)00278-8).
- Yu, S., Yin, L., Pang, H., Wu, Y., Wang, X., Zhang, P., Hu, B., Chen, Z., Wang, X., 2018a. Constructing sphere-like cobalt-molybdenum-nickel ternary hydroxide and calcined ternary oxide nanocomposites for efficient removal of U(VI) from aqueous solutions. *Chem. Eng. J.* 352, 360–370. <https://doi.org/10.1016/j.cej.2018.07.033>.
- Yu, S., Liu, Y., Ai, Y., Wang, X., Zhang, R., Chen, Z., Chen, Z., Zhao, G., Wang, X., 2018b. Rational design of carbonaceous nanofiber/Ni-Al layered double hydroxide nanocomposites for high-efficiency removal of heavy metals from aqueous solutions. *Environ. Pollut.* 242, 1–11. <https://doi.org/10.1016/j.envpol.2018.06.031>.
- Zhang, Y., Chi, H., Zhang, W., Sun, Y., Liang, Q., Gu, Y., Jing, R., 2014. Highly efficient adsorption of copper ions by a PVP-Reduced graphene oxide based on a new adsorptions mechanism. *Nano-Micro Lett.* 6, 80–87. <https://doi.org/10.1007/BF03353772>.